Advances in Civil Engineering

Novel Building Materials for Disaster Prevention and Mitigation

Lead Guest Editor: Zheng-zheng Wang
Guest Editors: Chunshun Zhang and Shengshan Pan

Novel Building Materials for Disaster Prevention and Mitigation

Novel Building Materials for Disaster Prevention and Mitigation

Lead Guest Editor: Zheng-zheng Wang
Guest Editors: Chunshun Zhang and Shengshan Pan

Zhaofei Chu, China
Wonseok Chung, Republic of Korea
Donato Ciampa, Italy
Gian Paolo Cimellaro, Italy
Francesco Colangelo, Italy
Romulus Costache, Romania
Liviu-Adrian Cotfas, Romania
Antonio Maria D'Altri, Italy
Bruno Dal Lago, Italy
Amos Darko, Hong Kong
Arka Jyoti Das, India
Dario De Domenico, Italy
Gianmarco De Felice, Italy
Stefano De Miranda, Italy
Maria T. De Risi, Italy
Tayfun Dede, Turkey
Sadik O. Degertekin, Turkey
Camelia Delcea, Romania
Cristoforo Demartino, China
Giuseppe Di Filippo, Italy
Luigi Di Sarno, Italy
Fabio Di Trapani, Italy
Aboelkasim Diab, Egypt
Thi My Dung Do, Vietnam
Giulio Dondi, Italy
Jiangfeng Dong, China
Chao Dou, China
Mario D'Aniello, Italy
Jingtao Du, China
Ahmed Elghazouli, United Kingdom
Francesco Fabbrocino, Italy
Flora Faleschini, Italy
Dingqiang Fan, Hong Kong
Xueping Fan, China
Qian Fang, China
Salar Farahmand-Tabar, Iran
Ilenia Farina, Italy
Roberto Fedele, Italy
Guang-Liang Feng, China
Luigi Fenu, Italy
Tiago Ferreira, Portugal
Marco Filippo Ferrotto, Italy
Antonio Formisano, Italy
Guoyang Fu, Australia
Stefano Galassi, Italy
Junfeng Gao, China
Meng Gao, China
Giovanni Garcea, Italy
Enrique García-Macías, Spain
Emilio García-Taengua, United Kingdom
DongDong Ge, USA
Khaled Ghaedi, Malaysia
Khaled Ghaedi, Malaysia
Gian Felice Giaccu, Italy
Agathoklis Giaralis, United Kingdom
Ravindran Gobinath, India
Rodrigo Gonçalves, Portugal
Peilin Gong, China
Belén González-Fonteboa, Spain
Salvatore Grasso, Italy
Fan Gu, USA
Erhan Güneyisi, Turkey
Esra Mete Güneyisi, Turkey
Pingye Guo, China
Ankit Gupta, India
Federico Gusella, Italy
Kemal Hacıefendioğlu, Turkey
Jianyong Han, China
Song Han, China
Asad Hanif, Macau
Hadi Hasanzadehshooiili, Canada
Mostafa Fahmi Hassanein, Egypt
Amir Ahmad Hedayat, Iran
Khandaker Hossain, Canada
Zahid Hossain, USA
Chao Hou, China
Biao Hu, China
Jiang Hu, China
Xiaodong Hu, China
Lei Huang, China
Cun Hui, China
Bon-Gang Hwang, Singapore
Jijo James, India
Abbas Fadhil Jasim, Iraq
Ahad Javanmardi, China
Krishnan Prabhakan Jaya, India
Dong-Sheng Jeng, Australia
Han-Yong Jeon, Republic of Korea
Pengjiao Jia, China
Shaohua Jiang, China

MOUSTAFA KASSEM, Malaysia
Mosbeh Kaloop, Egypt
Shankar Karuppannan, Ethiopia
John Kechagias, Greece
Mohammad Khajehzadeh, Iran
Afzal Husain Khan, Saudi Arabia
Mehran Khan, Hong Kong
Manoj Khandelwal, Australia
Jin Kook Kim, Republic of Korea
Woosuk Kim, Republic of Korea
Vaclav Koci, Czech Republic
Loke Kok Foong, Vietnam
Hailing Kong, China
Leonidas Alexandros Kouris, Greece
Kyriakos Kourousis, Ireland
Moacir Kripka, Brazil
Anupam Kumar, The Netherlands
Emma La Malfa Ribolla, Czech Republic
Ali Lakirouhani, Iran
Angus C. C. Lam, China
Thanh Quang Khai Lam, Vietnam
Luciano Lamberti, Italy
Andreas Lampropoulos, United Kingdom
Raffaele Landolfo, Italy
Massimo Latour, Italy
Bang Yeon Lee, Republic of Korea
Eul-Bum Lee, Republic of Korea
Zhen Lei, Canada
Leonardo Leonetti, Italy
Chun-Qing Li, Australia
Dongsheng Li, China
Gen Li, China
Jiale Li, China
Minghui Li, China
Qingchao Li, China
Shuang Yang Li, China
Sunwei Li, Hong Kong
Yajun Li, China
Shun Liang, China
Francesco Liguori, Italy
Jae-Han Lim, Republic of Korea
Jia-Rui Lin, China
Kun Lin, China
Shibin Lin, China
Tzu-Kang Lin, Taiwan
Yu-Cheng Lin, Taiwan
Hexu Liu, USA
Jian Lin Liu, China
Xiaoli Liu, China
Xuemei Liu, Australia
Zaobao Liu, China
Zhuang-Zhuang Liu, China
Diego Lopez-Garcia, Chile
Cristiano Loss, Canada
Lyan-Ywan Lu, Taiwan
Jin Luo, USA
Yanbin Luo, China
Jianjun Ma, China
Junwei Ma, China
Tian-Shou Ma, China
Zhongguo John Ma, USA
Maria Macchiaroli, Italy
Domenico Magisano, Italy
Reza Mahinroosta , Australia
Yann Malecot, France
Prabhat Kumar Mandal, India
John Mander, USA
Iman Mansouri, Iran
André Dias Martins, Portugal
Domagoj Matesan, Croatia
Jose Matos, Portugal
Vasant Matsagar, India
Claudio Mazzotti, Italy
Ahmed Mebarki, France
Gang Mei, China
Kasim Mermerdas, Turkey
Giovanni Minafò, Italy
Masoomeh Mirrashid, Iran
Abbas Mohajerani, Australia
Fadzli Mohamed Nazri, Malaysia
Fabrizio Mollaioli, Italy
Rosario Montuori, Italy
H. Naderpour, Iran
Hassan Nasir, Pakistan
Hossein Nassiraei, Iran
Satheeskumar Navaratnam, Australia
Ignacio J. Navarro, Spain
Ashish Kumar Nayak, India
Behzad Nematollahi, Australia

Chayut Ngamkhanong, Thailand
Trung Ngo, Australia
Tengfei Nian, China
Mehdi Nikoo, Canada
Youjun Ning, China
Olugbenga Timo Oladinrin, United Kingdom
Oladimeji Benedict Olalusi, South Africa
Timothy O. Olawumi, Hong Kong
Alejandro Orfila, Spain
Maurizio Orlando, Italy
Siti Aminah Osman, Malaysia
Walid Oueslati, Tunisia
SUVASH PAUL, Bangladesh
John-Paris Pantouvakis, Greece
Fabrizio Paolacci, Italy
Giuseppina Pappalardo, Italy
Fulvio Parisi, Italy
Dimitrios G. Pavlou, Norway
Daniele Pellegrini, Italy
Gatheeshgar Perampalam, United Kingdom
Daniele Perrone, Italy
Giuseppe Piccardo, Italy
Vagelis Plevris, Qatar
Andrea Pranno, Italy
Adolfo Preciado, Mexico
Chongchong Qi, China
Yu Qian, USA
Ying Qin, China
Giuseppe Quaranta, Italy
Krishanu ROY, New Zealand
Vlastimir Radonjanin, Serbia
Carlo Rainieri, Italy
Rahul V. Ralegaonkar, India
Raizal Saifulnaz Muhammad Rashid, Malaysia
Alessandro Rasulo, Italy
Chonghong Ren, China
Qing-Xin Ren, China
Dimitris Rizos, USA
Geoffrey W. Rodgers, New Zealand
Pier Paolo Rossi, Italy
Nicola Ruggieri, Italy
JUNLONG SHANG, Singapore
Nikhil Saboo, India
Anna Saetta, Italy
Juan Sagaseta, United Kingdom
Timo Saksala, Finland
Mostafa Salari, Canada
Ginevra Salerno, Italy
Evangelos J. Sapountzakis, Greece
Vassilis Sarhosis, United Kingdom
Navaratnarajah Sathiparan, Sri Lanka
Fabrizio Scozzese, Italy
Halil Sezen, USA
Payam Shafigh, Malaysia
M. Shahria Alam, Canada
Yi Shan, China
Hussein Sharaf, Iraq
Mostafa Sharifzadeh, Australia
Sanjay Kumar Shukla, Australia
Amir Si Larbi, France
Okan Sirin, Qatar
Piotr Smarzewski, Poland
Francesca Sollecito, Italy
Rui Song, China
Tian-Yi Song, Australia
Flavio Stochino, Italy
Mayank Sukhija, USA
Piti Sukontasukkul, Thailand
Jianping Sun, Singapore
Xiao Sun, China
T. Tafsirojjaman, Australia
Fujiao Tang, China
Patrick W.C. Tang, Australia
Zhi Cheng Tang, China
Weerachart Tangchirapat, Thailand
Xiaxin Tao, China
Piergiorgio Tataranni, Italy
Elisabete Teixeira, Portugal
Jorge Iván Tobón, Colombia
Jing-Zhong Tong, China
Francesco Trentadue, Italy
Antonello Troncone, Italy
Majbah Uddin, USA
Tariq Umar, United Kingdom
Muahmmad Usman, United Kingdom
Muhammad Usman, Pakistan
Mucteba Uysal, Turkey

Ilaria Venanzi, Italy
Castorina S. Vieira, Portugal
Valeria Vignali, Italy
Claudia Vitone, Italy
Liwei WEN, China
Chunfeng Wan, China
Hua-Ping Wan, China
Roman Wan-Wendner, Austria
Chaohui Wang, China
Hao Wang, USA
Shiming Wang, China
Wayne Yu Wang, United Kingdom
Wen-Da Wang, China
Xing Wang, China
Xiuling Wang, China
Zhenjun Wang, China
Xin-Jiang Wei, China
Tao Wen, China
Weiping Wen, China
Lei Weng, China
Chao Wu, United Kingdom
Jiangyu Wu, China
Wangjie Wu, China
Wenbing Wu, China
Zhixing Xiao, China
Gang Xu, China
Jian Xu, China
Panpan, China
Rongchao Xu, China
HE YONGLIANG, China
Michael Yam, Hong Kong
Hailu Yang, China
Xu-Xu Yang, China
Hui Yao, China
Xinyu Ye, China
Zhoujing Ye , China
Gürol Yildirim, Turkey
Dawei Yin, China
Doo-Yeol Yoo, Republic of Korea
Zhanping You, USA
Afshar A. Yousefi, Iran
Xinbao Yu, USA
Dongdong Yuan, China
Geun Y. Yun, Republic of Korea
Hyun-Do Yun, Republic of Korea
Cemal YİĞİT, Turkey
Paolo Zampieri, Italy
Giulio Zani, Italy
Mariano Angelo Zanini, Italy
Zhixiong Zeng, Hong Kong
Mustafa Zeybek, Turkey
Henglong Zhang, China
Jiupeng Zhang, China
Tingting Zhang, China
Zengping Zhang, China
Zetian Zhang, China
Zhigang Zhang, China
Zhipeng Zhao, Japan
Jun Zhao, China
Annan Zhou, Australia
Jia-wen Zhou, China
Hai-Tao Zhu, China
Peng Zhu, China
QuanJie Zhu, China
Wenjun Zhu, China
Marco Zucca, Italy
Haoran Zuo, Australia
Junqing Zuo, China
Robert Černý, Czech Republic
Süleyman İpek, Turkey

Contents

Hindawi
Advances in Civil Engineering
Volume 2021, Article ID 4537485, 5 pages
https://doi.org/10.1155/2021/4537485

Research Article

Displacement Approach to Determine the Effective Tensile and Torsional Modulus of Nanowires

Lin Fang,[1] Quan Yuan ,[2] Bin Wu,[3] Honglin Li,[4] and Mengyang Huang[2]

[1]*China Merchants Chongqing Communications Research & Design Institute Co., Ltd., Chongqing 400067, China*
[2]*School of Civil Engineering, Architecture and Environment, Xihua University, Hongguang Town, Chengdu 610039, China*
[3]*Sichuan Yakang Expressway Co., Ltd., Ya'an 625000, China*
[4]*China Railway Construction Bridge Engineering Bureau Group 3rd Engineering Co., Shenyang 110043, China*

Correspondence should be addressed to Quan Yuan; yuanqxh@163.com

Received 17 May 2021; Accepted 7 September 2021; Published 22 September 2021

Academic Editor: Zheng-Zheng Wang

Surface elasticity and residual stress have a strong influence on the effective properties of nanowire (NW) due to its excessively large surface area-to-volume ratio. Here, the classical displacement method is used to solve the field equations of the core-surface layer model subjected to tension and torsion. The effective Young's modulus is defined as the ratio of normal stress to axial strain, which decreases with the increase in NW radius and gradually reaches the bulk value. The positive or negative surface residual stresses will increase or decrease Young's modulus and shear modulus due to the surface residual strains. Nonzero radial and circumferential strains enhance the influence of surface moduli on the effective modulus.

1. Introduction

Typical nanowires (NWs) are often referred to as 1D materials with nanometer-scale diameters or perimeters and excessively large surface area-to-volume ratio. NWs have considerable potential in various applications, such as molecular electronics, nanoelectromechanical systems, and novel building materials, for disaster prevention and mitigation [1–12]. The applications of NWs into future generation nanodevices require a complete understanding of the NW mechanical properties [2]. Many direct measurements have been performed to investigate the mechanical properties of NWs [3]. Unlike the mechanical testing of bulk materials, NW testing heavily depends on the experimental setup; in particular, manipulation procedure leads to substantial challenges due to the small NW dimensions [4]. In many experiments, such as in [1–6], the measured deflections are less than the diameter which can be classified small-deflection problem. In addition to experimental endeavors, theoretical prediction can also be used in NW mechanical analysis. Theoretical prediction is classified into two main categories as follows: first is the atomic modeling, which includes techniques such as tedious *ab initio* molecular dynamics calculations and density functional model [5], and second one is continuum mechanics modeling [6–10]. NWs are strongly influenced by their surface characteristics, thereby leading to distinct mechanical properties compared with their bulk counterpart. Consequently, in the continuum mechanics modeling of the mechanical properties of a solid NW, the role of surface stress must be considered. Zhang et al. analyzed the effect of surface residual stress and elasticity on the asymmetric yield strength of NWs on the basis of the potential energy method [6]. Chuang presented a simplistic theory to study the enhanced strength of a solid NW [7]. Gupta also presented a continuum formulation to investigate the finite deformation of nanorod/NWs [8]. The large-deflection deformation of NW implicates large rotational angle and infinitesimal strain. So, this situation will not be considered in our mode.

Although the classical continuum mechanics models can efficiently predict NW deformation, their applicability in identifying the surface effect on the effective modulus of NWs is tedious. Therefore, a relatively simple approach that can directly characterize the mechanical properties of a solid NW should be developed. In this work, the classical displacement method is used to study the tension and torsion of

NW and the influence of surface elasticity on the effective Young's moduli and shear moduli.

2. Model Analysis

As schematically shown in Figure 1, we consider a stretched and twisted core-shell NW model viewed as a composite, comprising a cylindrical core (bulk) and surface layer. The equilibrium equations, strain-displacement relationships, and constitutive equations for the isotropic bulk materials are expressed as follows:

$$\varepsilon_{ij} = \frac{1}{2}\left(u_{i,j} + u_{j,i}\right), \tag{1}$$

$$\sigma_{ij} = \lambda\varepsilon_{kk}\delta_{ij} + 2G\varepsilon_{ij}, \tag{2}$$

$$\sigma_{ij,j} = 0, \tag{3}$$

where σ_{ij}, u_i, and ε_{ij} denote the stresses, displacements, and strains in core, respectively, and λ and G are the Lamé constants of the bulk. For the elastic isotropic surface layer, the linear relationship of the surface stress and elastic strain can be expressed by Gurtin–Murdoch elasticity as follows [9]:

$$\tau^s_{\alpha\beta} = \tau_0\delta_{\alpha\beta} + \lambda_s\varepsilon^s_{\chi\chi}\delta_{\alpha\beta} + 2G_s\varepsilon^s_{\alpha\beta}, \tag{4}$$

where λ_s and G_s are the surface modulus, τ_0 is the surface residual stress, and $\delta_{\alpha\beta}$ denotes the surface Christoffel symbols. According to the analysis of the mechanical equilibrium of surface layer and core, the generalized Young–Laplace equations for NW are expressed as follows [6, 10]:

$$\sigma_{\alpha j}n_j + \tau^s_{\alpha\beta,\beta} = 0, \tag{5}$$

$$\sigma_{ij}n_jn_i = \tau^s_{\alpha\beta}\kappa^s_{\alpha\beta}, \tag{6}$$

where n_j is the unit normal vector and $\kappa^s_{\alpha\beta}$ is the curvature tensor of the surface (Figure 2). The stress distribution of NW can be obtained using the classical displacement method on the basis of equations (1)~(6), that is, the bulk stress and the surface stress can be obtained by directly substituting the bulk displacement/strain formula into the constitutive equations. The global displacements dominant governing equations are established using generalized Young–Laplace equations. The solution of the field equations in the cylinder coordinate can be simplified if the NW is subjected to tension and torsion. We assume that u_z is function of z and u_ρ is function of ρ. According to equation (1), the nonzero strains are

$$\begin{aligned}
\varepsilon_z &= \frac{du_z}{dz},\\
\varepsilon_\rho &= \frac{du_\rho}{d\rho}r,\\
\varepsilon_\varphi &= \frac{u_\rho}{\rho},\\
\gamma_{z\varphi} &= \frac{\partial u_\varphi}{\partial z}.
\end{aligned} \tag{7}$$

After substituting equation (7) into equation (2), the stress components in the bulk are

$$\sigma_\rho = (\lambda + 2G)\frac{du_\rho}{d\rho} + \lambda\frac{du_z}{dz} + \lambda\frac{u_\rho}{\rho}, \tag{8}$$

$$\sigma_\varphi = (\lambda + 2G)\frac{u_\rho}{\rho} + \lambda\frac{du_z}{dz} + \lambda\frac{du_\rho}{d\rho}, \tag{9}$$

$$\sigma_z = (\lambda + 2G)\frac{du_z}{dz} + \lambda\frac{u_\rho}{\rho} + \lambda\frac{du_\rho}{d\rho}, \tag{10}$$

$$\tau_{z\varphi} = G\gamma_{z\varphi}. \tag{11}$$

After substituting equations (8)–(11) into equation (3), it is noted that $\sigma_\rho = \sigma_\varphi$, and the stress components are found to be automatically satisfied the radial equilibrium equation. And, we get $\varepsilon_\rho = \varepsilon_\varphi$ and u_ρ is the linear distribution along the radial direction. The axial and circumferential equilibrium equation can be simplified into the following forms:

$$\frac{d^2u_z}{dz^2} = 0, \tag{12}$$

$$\frac{\partial^2u_\varphi}{\partial\varphi^2} = 0, \tag{13}$$

which implies that u_z and u_φ are linear distribution along the axial direction of NW. Now, the displacement field can be expressed by

$$u_\varphi = \rho\left(a_1z + b_1\right), \tag{14}$$

$$u_z = a_2z + b_2, \tag{15}$$

$$u_\rho = a_3\rho, \tag{16}$$

where $a_1 \sim a_3$ and $b_1 \sim b_2$ are constants related to boundary conditions. The surface of NW is assumed to be characterized by the deformation of the bulk solid so that surface strains can be expressed by

$$\begin{aligned}
\varepsilon^s_{zz} &= a_2,\\
\varepsilon^s_{\varphi\varphi} &= a_3,\\
\gamma^s_{z\varphi} &= R_0a_1,
\end{aligned} \tag{17}$$

where R_0 is the radius of NW. Substituting equation (17) into equation (4), the surface stresses are

$$\tau^s_{zz} = \tau_0 + \left(\lambda_s + 2G_s\right)a_2 + \lambda_sa_3, \tag{18}$$

$$\tau^s_{\varphi\varphi} = \tau_0 + \left(\lambda_s + 2G_s\right)a_3 + \lambda_sa_2, \tag{19}$$

$$\tau^s_{z\varphi} = G_sR_0a_1. \tag{20}$$

After substituting equations (18)–(20) into equations (5) and (6), the above surface stress components automatically satisfy the axial and circumferential generalized

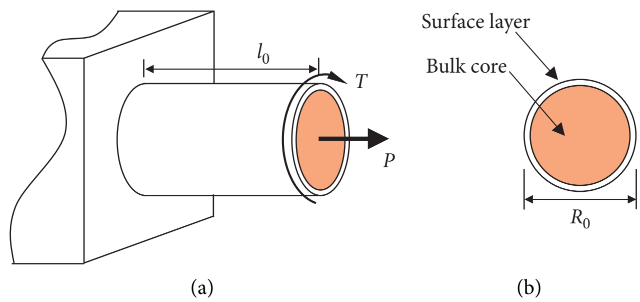

FIGURE 1: Core-surface layer model of NW. (a) Tension and torsion of NW. (b) Cross section of NW.

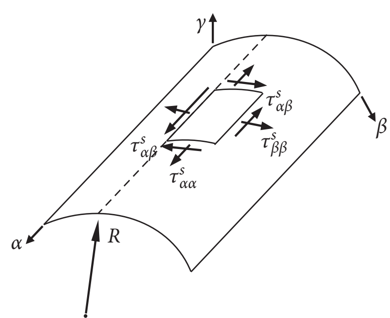

FIGURE 2: Elementary surface layer.

Young–Laplace equations. The generalized Young–Laplace equation along the radial direction gives $\sigma_p = \tau^s_{\varphi\varphi}/R_0$, and it is

$$a_3 = -\frac{\left(\lambda + \lambda_p\right)a_2}{2(\lambda + G) + \lambda_p + 2G_p}. \tag{21}$$

Under a constant external load P, the average normal stress on the cross section of NW is

$$\bar{\sigma} = \frac{P}{\pi R_0^2} = \frac{2\tau_0}{R_0} + \left[(\lambda + 2G) + 2\left(\lambda_p + 2G_p\right)\right]a_2 + 2\left(\lambda + \lambda_p\right)a_3, \tag{22}$$

where $\lambda_p = \lambda_s/R_0$ and $G_p = G_s/R_0$. Under a constant external torsion T, the shear stress on the cross section of NW satisfy the following equation:

$$\left(GI_p + G_s I_s\right)a_1 = T, \tag{23}$$

where $I_p = \pi R_0^4/32$ and $I_s = 2\pi R_0^3$. Combining equations (17), (22), and (23), the constants can be confirmed as follows:

$$a_1 = \frac{T}{GI_p + G_s I_s}, \tag{24}$$

$$a_2 = \frac{\left(\bar{\sigma} - \left(2\tau_0/R_0\right)\right)\left(2\lambda + 2G + \lambda_p + 2G_p\right)}{2G(2G + 3\lambda) + \lambda_P(6G + \lambda) + 2G_p\left(6G + 5\lambda + 4G_p + 4\lambda_p\right)}, \tag{25}$$

$$a_3 = -\frac{-\left(\bar{\sigma} - \left(2\tau_0/R_0\right)\right)\left(\lambda + \lambda_p\right)}{2G(2G + 3\lambda) + \lambda_P(6G + \lambda) + 2G_p\left(6G + 5\lambda + 4G_p + 4\lambda_p\right)}. \tag{26}$$

We next determine the distribution of the surface residual strain and then consider the effective modulus of NW. If nonzero surface residual stress is present on the NW surface and let $\bar{\sigma} = 0$ in equations (25) and (26), then the relaxed surface axial strain and circumferential strain are expressed as follows:

$$\begin{aligned}
\varepsilon^s_{zz0} &= \frac{\left(-2\tau_0/R_0\right)\left(2\lambda + 2G + \lambda_p + 2G_p\right)}{2G(2G + 3\lambda) + \lambda_P(6G + \lambda) + 2G_p\left(6G + 5\lambda + 4G_p + 4\lambda_p\right)}, \\
\varepsilon^s_{\varphi\varphi0} &= \frac{\left(-2\tau_0/R_0\right)\left(\lambda + \lambda_p\right)}{2G(2G + 3\lambda) + \lambda_P(6G + \lambda) + 2G_p\left(6G + 5\lambda + 4G_p + 4\lambda_p\right)}.
\end{aligned} \tag{27}$$

The surface residual stresses of the NW are inherent and in the self-equilibrium state, that is, independent of the external load. If the NW is subjected to tension and torsion, then the strain and stress analysis of NW can be also performed using equations (7)~(26). Let u_{z0} and u_{zl} be the axial displacements of the two NW ends and l_0 be the initial length of NW; the average axial strain is

$$\bar{\varepsilon} = \frac{u_{zl} - u_{z0}}{l_0} = a_2. \tag{28}$$

The effective strains of NW are the difference between average axial strain and surface radial strain, as expressed below:

$$\begin{aligned} \varepsilon_{z\mathrm{eff}} &= \bar{\varepsilon}_{zz} - \varepsilon^{s}_{zz0}, \\ \varepsilon_{\varphi\mathrm{eff}} &= \bar{\varepsilon}_{\varphi\varphi} - \varepsilon^{s}_{zz0}. \end{aligned} \tag{29}$$

Consequently, the effective Young's modulus of NW is obtained as follows:

$$E_{\mathrm{eff}} = \frac{\bar{\sigma}}{\varepsilon_{z\mathrm{eff}}} = \frac{2G(2G+3\lambda) + \lambda_P(6G+\lambda) + 2G_p\left(6G+5\lambda+4G_p+4\lambda_p\right)}{2\lambda+2G+\lambda_p+2G_p}. \tag{30}$$

The effective Poisson's ratio of NW is

$$E_{\mathrm{eff}} = -\frac{a_3}{a_2} = \frac{\lambda+\lambda_p}{2\lambda+2G+\lambda_p+2G_p}. \tag{31}$$

The effective shear modulus of NW is

$$G_{\mathrm{eff}} = \frac{T}{I_p a_1} = G + \frac{G_s I_s}{I_p}. \tag{32}$$

3. Results and Discussion

All the displacements, strains, bulk stresses, and surface stresses of the NW have been determined using the classical displacement approach. Figure 3 shows the variation in the effective Young's moduli of the NW compared with its radius. For example, in Al NW, the surface moduli are $\lambda_s = 6.8415$ N/m and $G_s = -0.3755$ N/m [6]. The bulk parameters are $\lambda = 59.2$ GPa and $G = 25.4$ GPa [6]. The solid curve on the basis of our continuum formula (equation (16)) matches Zhang et al. [6] approach (the dotted curve). The effect of surface stresses on the effective Young's modulus of NW is illustrated, where Young's modulus decreases with the increase in the NW radius (R_0) and gradually reaches a constant value of 69 GPa. As shown in Figure 3, the two approaches provide slightly different results with small radius (<5 nm). Our formula offers small effective Young' modulus and rapid reduction because the potential energy method adds to the influence of radial and circumferential strains in the definition of Young's modulus. Homogenization theory of nanocomposites can provide a rigorous definition to define effective properties [10]. As depicted in equation (28), the surface residual stresses (τ_0) also affects Young's modulus. The surface residual stresses are inherent and in the self-equilibrium state, that is, independent of the external load, due to the surface residual strain (equation [10]). Hence, the positive or negative surface residual stresses will increase (or decrease) Young's modulus of NW.

Surface moduli also have strong influence on Young's modulus. The absolute value of the NW surface elasticity is generally <1000 N/m, but it is difficult to accurately quantify. A minimal difference is observed between the experimental approach and numerical atomistic analysis even with small radius. For reference, we also present the variation of the effective modulus of NW compared with its surface moduli in Figure 4. The NW with a large radius is considered ($R = 10$ nm, 20 nm, 30 nm, 40 nm) solely for computational purpose. Figure 4 illustrates the increase in Young's modulus with the increase in the surface moduli (λ_s). Equations (8)–(11) show that the surface shear strains are zero, but the surface area expansion is nonzero. Equation (4) implies high surface stress values with high surface moduli, thereby resulting in large NW Young's modulus. However, the amplification of the surface moduli on Young's modulus is controlled by the NW radius, that is, the surface area-to-volume ratio increases with the decrease in NW radius. This result suggested that the effective modulus of NW is enhanced by the surface stress. Size dependence is the general characteristics of nanomaterials. Classical displacement approach can provide the surface strain and stress and simplifies the analysis of the effect of surface elasticity on Young's modulus.

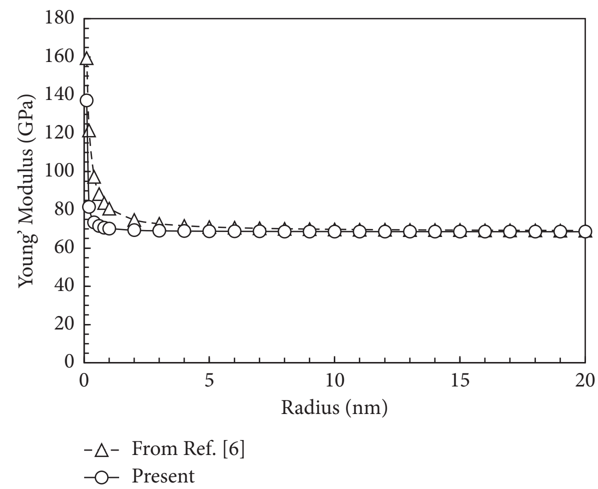

Figure 3: Young's modulus of NW vs. radius.

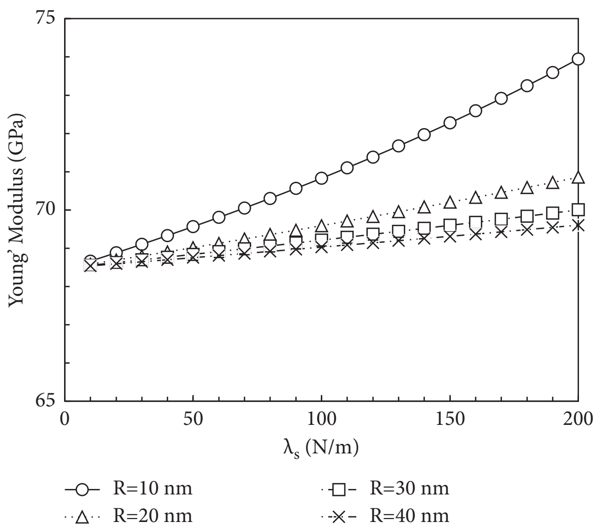

FIGURE 4: Young's modulus of NW vs. surface moduli.

4. Conclusions

NW can be viewed as a composite structure, with the inner core having the normal properties and the surface layer having surface elasticity on the basis of the Gurtin–Murdoch elasticity. The generalized Young–Laplace equations for NW are required in addition to the field equations for core and surface layer. Classical displacement approach in the cylinder coordinate has been used to determine the stress distribution of NW. The nominal normal stress and axial strain are defined in the initial NW configuration with initial length (l_0) and radius (R_0). The l_0/R_0 ratio shows that the effective Young's modulus decreases with the increase in R_0 of the nanowire and gradually reaches the bulk value. The positive or negative surface residual stresses will increase (or decrease) Young's modulus of NW due to the surface residual strain. Surface moduli also have strong influence on the effective Young's modulus. Nonzero radial and circumferential strains lead to nonzero area expansion, which enhances the influence of surface moduli effective Young's modulus.

The radial displacement in the NW is finite [8], and the present model can be easily extended to analyze the effective properties if true strain is used. NW torsion and bending may also be modeled if we consider a proper assumption of the displacement distribution in equation (7). In conclusion, classical displacement approach can obtain NW displacements, strains, and stress distributions and as well as its effective properties. The mechanism underlying the influence of the general characteristics of NW on Young's modulus can also be easily considered.

Data Availability

The cited data, about surface elastic constants of silver nanowire, used to support the findings of this study are included within the article. The data have been used to verify our theoretical prediction.

Conflicts of Interest

The authors declare that they have no conflicts of interest.

Acknowledgments

The authors gratefully acknowledge the financial supports to this work from the National Engineering Laboratory for Highway Tunnel Construction Technology (Grant no. NELFHT201702), the Chunhui project of Ministry of Education of the People's Republic of China (Grant no. z2014040), Research Project of Sichuan Provincial Department of Education (Grant no. 15ZA0138), and Key Research Project of Xihua University (Grant no. z1320608).

References

[1] D. Appell, "Wired for success," *Nature*, vol. 419, no. 6907, pp. 553–555, 2002.

[2] E. Gil-Santos, D. Ramos, J. Martínez et al., "Nanomechanical mass sensing and stiffness spectrometry based on two-dimensional vibrations of resonant nanowires," *Nature Nanotechnology*, vol. 5, no. 9, pp. 641–645, 2010.

[3] S. Ding, Y. H. Tian, Z. Jiang, and X. B. He, "Molecular dynamics simulation of joining process of Ag-Au nanowires and mechanical properties of the hybrid nanojoint," *AIP Advances*, vol. 5, no. 5, pp. 057120-1–57210, 2015.

[4] S. Wang, Z. Shan, and H. Huang, "The mechanical properties of nanowires," *Advanced Science*, vol. 4, no. 4, pp. 1600332–1600341-24, 2017.

[5] M. Friak, M. Sob, and V. Vitek, "Ab initio study of the ideal tensile strength and mechanical stability of transition-metal disilicides," *Physical Review B*, vol. 68, no. 68, pp. 380–383, 2003.

[6] W. Zhang, T. Wang, and X. Chen, "Effect of surface stress on the asymmetric yield strength of nanowires," *Journal of Applied Physics*, vol. 103, no. 12, pp. 123527–123531-5, 2008.

[7] T. J. Chuang, P. M. Anderson, M. K. Wu, and S. Hsieh, *Nanomechanics of Materials and Structures*, p. 67, Springer, Berlin/Heidelberg, Germany, 2006.

[8] P. Gupta and A. Kumar, "Effect of surface elasticity on extensional and torsional stiffnesses of isotropic circular nanorods," *Mathematics and Mechanics of Solids*, vol. 24, no. 6, pp. 1613–1629, 2019.

[9] M. E. Gurtin and A. Ian Murdoch, "Surface stress in solids," *International Journal of Solids and Structures*, vol. 14, no. 6, pp. 431–440, 1978.

[10] H. L. Duan, J. Wang, Z. P. Huang, and B. L. Karihaloo, "Size-dependent effective elastic constants of solids containing nano-inhomogeneities with interface stress," *Journal of the Mechanics and Physics of Solids*, vol. 53, no. 7, pp. 1574–1596, 2005.

[11] X. L. Weng, R. M. Zhou, W. Rao, and D. Wang, "Research on subway shield tunnel induced by local water immersion of collapsible loess," *Natural Hazards*, vol. 108, pp. 1197–1219, 2021.

[12] Y. F. Yan, J. L. Qiu, and Q. B. Huang, "Ground fissures geology in Xi'an and failure mitigation measures for utility tunnel system due to geohazard," *Arabian Journal of Geosciences*, vol. 14, 2021.

Hindawi
Advances in Civil Engineering
Volume 2021, Article ID 6726685, 5 pages
https://doi.org/10.1155/2021/6726685

Research Article

Effect of Curvature-Dependent Surface Elasticity on the Flexural Properties of Nanowire

Mengjun Wu,[1] Quan Yuan ,[2] Honglin Li ,[3] Bin Wu ,[4] Lin Fang,[1] and Mengyang Huang[2]

[1]*China Merchants Chongqing Communications Research & Design Institute Co., Ltd., Chongqing 400067, China*
[2]*School of Civil Engineering, Architecture and Environment, Xihua University, Hongguang Town, Chengdu 610039, China*
[3]*China Railway Constructionbridge Engineering Bureau Group 3rd Engineering Co., Shenyang 110043, China*
[4]*Sichuan Yakang Expressway Co., Ltd., Ya'an 625000, China*

Correspondence should be addressed to Quan Yuan; yuanqxh@163.com

Received 28 May 2021; Accepted 14 July 2021; Published 27 July 2021

Academic Editor: Zheng-zheng Wang

Surface elasticity and residual stress strongly influence the flexural properties of nanowire due to the excessively large ratio of surface area to volume. In this work, we adopt linearized surface elasticity theory, which was proposed by Chhapadia et al., to capture the influence of surface curvature on the flexural rigidity of nanowire with rectangular cross section. Additionally, we have tried to study the bending deformation of circular nanowire. All stresses and strains are measured relative to the relaxed state in which the difference in surface residual stress between the upper and lower faces of rectangular nanowire with no external load induces additional bending. The bending curvature of nanowire in the reference and relaxed states is obtained. We find that flexural rigidity is composed of three parts. The first term is defined by the precept of continuum mechanics, and the last two terms are defined by surface elasticity. The normalized curvature increases with the decrease in height, thereby stiffening the nanowire. We also find that not only sizes but also surface curvature induced by surface residual stress influence the bending rigidity of nanowire.

1. Introduction

The effect of surface/interface elasticity on the mechanical properties of one-dimensional nanostructures, particularly those of nanowires, has attracted widespread interest [1, 2]. The equilibrium position and free energy of surface/interface atoms are different from those of internal atoms, and the differences should be considered in predicting the size-dependent elastic properties of nanowire due to the large ratio of surface area to volume. The extensional and flexural properties are strongly affected by the surface characteristics. Three methods have been used to reveal the surface effects. Continuum mechanics formulation provides a global expression for the combination of surface elasticity and bulk deformation, and the defined surface parameters are determined by atomistic calculation or experiments [3].

Gurtin and Ian Murdoch (GM) were the first to establish rigorous mechanics to model the surface elasticity [4]. Miller and Shenoy studied the size-dependent effective stiffness properties of nanosized bar and beams using a core-shell model [5]. Zhang et al. estimated the effect of surface stress on the effective elastic modulus and asymmetric yield strength of nanowire [6]. Wang and Feng presented a theoretical model for investigating the effect of surface elasticity and residual surface tension on the natural frequency of nanobeam [7]. Xu et al. improved a core-shell model composed of a core and a surface shell layer with constant thickness to predict the effective elastic modulus of nanowire under tension and bending [8]. However, the intrinsic flexural resistance of the surface is ignored in the aforementioned model. The surface energy of nanowire should depend not only on the surface strain but also on the surface curvature. Steignmann and Ogden (SO) established a more general model for surface energy; this model depends on surface curvature in addition to in-plane stretch and shear [9]. Chhapadia et al. provided a simplified and linearized version of the model to study the influences of curvature dependence of surface energy on the effective elastic modulus of a thin cantilever beam under pure bending [10]. Gao et al. proposed a curvature-dependent interface energy function to study the nature of the interface stress and bending moment in a nanostructure [11].

The two most studied types of cross section of nanowire are the rectangular and circular sections. Circular nanowire with no external load may also present surface residual and couple stresses due to the initial curvature. The extensional properties of circular nanowire have been discussed in detail in [12, 13]. Rectangular nanowire represents different mechanisms on the surface from the circular nanowire. The nonuniform surface residual stress may induce the bending of nanowire, which corresponds to a relaxed state. Plane upper and lower surfaces will have a relaxation bending curvature that occupies a part of the surface energy. In this work, simple beam theory and the GM and SO models are adopted to predict the flexural properties of rectangular nanowire.

2. Model Analysis

In this section, the reference state of nanowire shown in Figure 1 is considered. The nanowire has four faces, namely, the upper surface, the lower surface, and two profile surfaces. The nanowire has thickness h, width b, and length l. h defines the size of nanowire. The definition of surface parameters depends on the constitutive relationship of nanowire, which is obscure in surface/interface mechanics. The hyperelastic model is the most commonly used constitutive model in which the surface energy density can be expressed by a function of the invariants of surface strain and relative curvature tensors [9, 12]. The derived relationship among surface stress, surface strain, and curvature denotes the usual nonlinear elasticity. In particular, a linearized curvature-dependent surface elasticity can be obtained for the infinitesimal deformation of nanowire [9]. Miller and Shenoy adopted Timoshenko's symmetric bending theory to obtain the surface stress difference between the upper and lower surfaces [5]. Chhapadia et al. provided a correction of curvature dependence of surface to Stoney's formula [10]. The constructions are defined in the reference or undeformed state of nanowire. However, the difference in surface residual stress between the upper and lower faces of nanowire with no external load may induce additional bending, which corresponds to a relaxation state. All stresses and strains in the nanowire will be measured relative to this state.

Following Chhapadia's formulation, only surface tension and compression along the axial direction on the upper and lower surfaces are considered, and they are assumed to be uniform along the width direction. The surface stresses can be expressed by

$$\begin{cases} \tau_{su} = \tau_{su0} + b_{su}\varepsilon_{su}, \\ \tau_{sl} = \tau_{sl0} + b_{sl}\varepsilon_{sl}, \end{cases} \tag{1}$$

where τ_{su0} and τ_{sl0} denote the surface residual stresses on the upper and lower surfaces, respectively; ε_{su} and ε_{sl} denote the surface strains; and b_{su} and τ_{sl0} are the material constants associated with surface strains. Under a constant bending moment M, the axial strain in bulk is given by

$$\varepsilon_x = -\kappa_y\left(y - h_y\right), \tag{2}$$

where κ_y is the bending curvature of nanowire and h_y is the height of neutral axis from the lower surface. The surface strains are determined by the axial strain at $y = 0$ and $y = h$. Thus, we have

$$\begin{cases} \varepsilon_{su} = -\kappa_y\left(h - h_y\right), \\ \varepsilon_{su} = \kappa_y h_y. \end{cases} \tag{3}$$

We assume that the residual stain in bulk in the relaxed state is linearly distributed along the height direction. Thus, we have

$$\varepsilon_{x0} = -\kappa_{y0}\left(y - h_{y0}\right), \tag{4}$$

where κ_{y0} is the relaxation curvature of nanowire and h_{y0} is the height of neutral axis in the reference state. Therefore, the stress in the bulk is given by

$$\sigma_x = E\left(\varepsilon_x - \varepsilon_{x0}\right), \tag{5}$$

where E is the elastic modulus of bulk material. For the upper and lower surface layers, the surface couple is given by

$$\begin{cases} m_{su} = C_u\left(\kappa_y - \kappa_{y0}\right), \\ m_{sl} = C_l\left(\kappa_y - \kappa_{y0}\right), \end{cases} \tag{6}$$

where C_u and C_l are the SO constants. We can establish the equilibrium equations by using the internal force balance of simple beam with the effect of surface stress. Surface stress, surface couple stress, and stress in bulk balance the applied moment M, and the integration over the cross-sectional area yields

$$\int_0^h \sigma_x (h - y) b\,dy + hb\tau_{sl} + b\left(m_{su} + m_{sl}\right) = M. \tag{7}$$

Thus, we have

$$\kappa_y = \frac{M + \left[Ebh^2\left(3h_{y0} - h\right)/6 + b\left(C_u + C_l\right)\right] - bh\tau_{sl0}}{Ebh^2\left(3h_y - h\right)/6 + b_{sl}bhh_y + b\left(C_u + C_l\right)}. \tag{8}$$

We balance the force, that is,

$$\int_0^h \sigma_x dy + \tau_{su} + \tau_{sl} = 0, \tag{9}$$

which gives us

$$h_y = \frac{\kappa_y h\left(Eh/2 + b_{su}\right) + \kappa_{y0}Eh\left(h_{y0} - h/2\right) - \left(\tau_{sl0} + \tau_{su0}\right)}{\kappa_y\left(Eh + b_{su} + b_{sl}\right)}. \tag{10}$$

If the surface stress emerges on the front and back surfaces by repeating the analysis of the preceding few pages, then the strains and stresses on the surfaces and in the bulk can be obtained. We now consider the curvature of nanowire

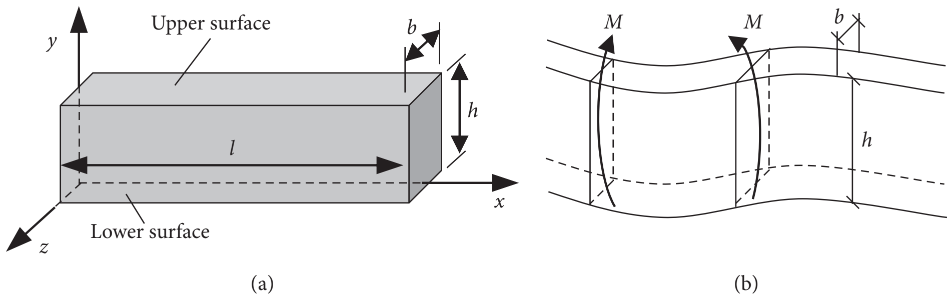

Figure 1: Configuration of nanowire. (a) Reference configuration. (b) Relaxation configuration.

in the relaxed state. We can use equations (8) and (10) to obtain the curvature at which the bending moment vanishes. We let $M = 0$ and $\kappa_y = 0$. Thus, we have

$$h_{y0} = \frac{\tau_{\mathrm{su0}} + \tau_{\mathrm{sl0}}}{E\kappa_{y0}} + \frac{h}{2}, \tag{11}$$

where h_{y0} is the height of neutral axis and is measured in the reference state. By substituting equation (11) into equation (8), we obtain

$$\kappa_{y0} = \frac{h\tau_{\mathrm{sl0}}}{Eh^2\left(3h_{y0} - h\right)/6 + C_u + C_l} = \frac{6h\Delta\tau_{s0}}{Eh^3 + 12\left(C_u + C_l\right)}, \tag{12}$$

where $\Delta\tau_{s0} = \tau_{\mathrm{sl0}} - \tau_{\mathrm{su0}}$. The above equation gives the same expression as Chhapadia's.

But for circular nanowire, the surface property is more complicated than that of rectangular nanowire. There is no two-dimensional periodicity on the cylindrical surface. The surface presents strong anisotropy. It is difficult to determine the surface elastic constants. The deformation in bulk induced by surface residual stress is still unclear. To qualitatively analyze the flexural properties of circular nanowire, we consider an isotropic surface without residual stress. For simplicity, the x axis is placed at the axial line of nanowire. Essentially repeating the analysis of the rectangular nanowire, the stress in the bulk is given by

$$\sigma_x = -E\kappa_y y. \tag{13}$$

The above equation is derived by letting $h_y = d/2$ and $\kappa_{y0} = 0$ in equation (5). The surface strain is

$$\varepsilon_s = -\frac{\kappa_y d \sin\varphi}{2}, \tag{14}$$

where φ is the polar angle on the cross section of nanowire. There are two curvatures on the cylindrical surface after the deformation of nanowire. One is $d/2$ which is independent of the deformation. The other curvature is κ_y. The surface stress and surface moment stress are

$$\begin{aligned} \tau_s &= C_0\varepsilon_s, \\ m_s &= C_1\kappa_s. \end{aligned} \tag{15}$$

Similarly balancing the moment, we have

$$\kappa_y = \frac{M}{EI_z + C_0 I_s + C_1 S}, \tag{16}$$

where $I_z = \pi d^4/64$ is the moment of inertia of the beam cross section, $I_s = \pi d^3/8$ is the perimeter moment of inertia, and $S = \pi d$. The effective bending rigidity is defined as

$$E^* I_z = EI_z + C_0 I_s + C_1 S, \tag{17}$$

where E^* is the effective elastic modulus. Equation (16) can be rewritten as

$$\kappa_y = \frac{M}{E^* I_z} = \frac{M}{EI_z\left(1 + 8C_0/dE + 64C_1/d^3E\right)}. \tag{18}$$

We see that the surface elasticity has a definite influence on the bending rigidity of circular nanowire.

3. Results and Discussion

We compare the curvature changes in the relaxed and pure bending moment loading states to explain the influence of curvature-dependent surface elasticity on the flexural properties of nanowire clearly. Chhapadia et al. [10] carried out an atomistic simulation of a silver nanowire with a thickness ranging from 1.6 nm to 6 nm. They found that $C_u = C_l = C$, $b_{\mathrm{su}} = b_{\mathrm{sl}} = b$, $C = -42.3155\,\mathrm{eV}$, and $b = -0.37938\,\mathrm{eV/Å^2}$ for the $\langle 1\,0\,0\rangle$ axially oriented nanowire, and $C = 114.1895\,\mathrm{eV}$ and $b = 2.5227\,\mathrm{eV/Å^2}$ for the $\langle 1\,1\,0\rangle$ axially oriented nanowire. The effective elastic constants for the $\langle 1\,0\,0\rangle$ surface orientations are negative, thereby softening the nanowire. Only the surface couple stresses on the upper and lower surfaces are considered in this discussion. The configuration of the nanowire is set to be $\langle 1\,1\,0\rangle$ axially, and the positive constants are adopted here.

Figure 2 presents the normalized curvature of nanowire $(\kappa_{y0}/(6\Delta\tau_{s0}/Eh^2)$ versus the height in the relaxed state. The normalized curvature without SO correction ($C = 0$) does not vary with the change in height, whereas the normalized curvature with SO correction decreases with the decrease in height. This condition implies that the relative stiffness of nanowire increases with the increase in height. The positive SO constant C induces additional surface energy, thereby

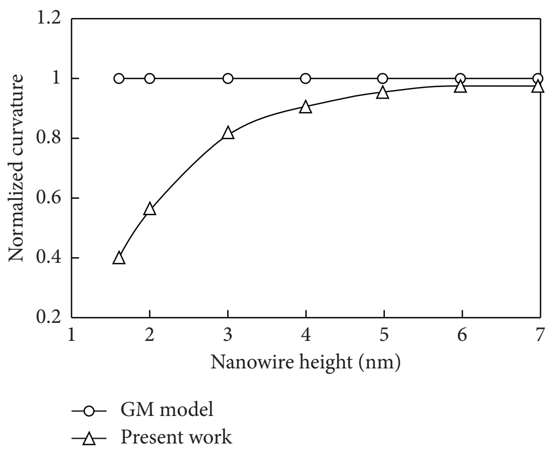

Figure 2: Curvature of ⟨110⟩ axially oriented silver nanowire in reference state.

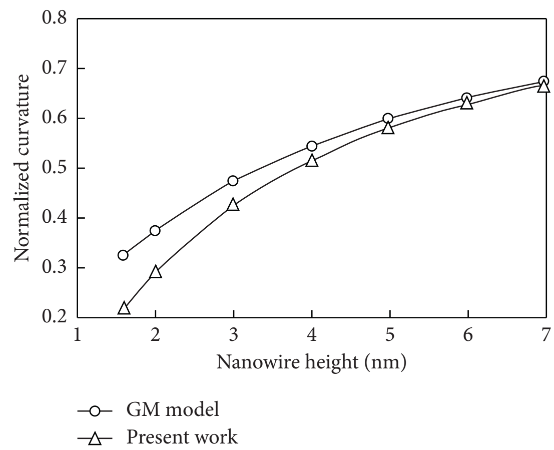

Figure 3: Curvature of ⟨110⟩ axially oriented silver nanowire in relaxed state.

stiffening the nanowire. Thus, the negative SO constant has a softening influence on the ⟨1 0 0⟩ axially oriented nanowire. Notably, the difference in surface residual stress on the upper and lower surfaces induces the relaxation curvature of nanowire. If $\Delta\tau_{s0} = 0$, that is, $\tau_{\mathrm{su}0} = \tau_{\mathrm{sl}0}$, then equation (12) shows that $\kappa_{y0} = 0$, and no bending deformation emerges in the relaxed state. The height of neutral axis h_{y0} has no meaning in such a case. If $\Delta\tau_{s0} = 2\tau_{\mathrm{sl}0}$, that is, $\tau_{\mathrm{su}0} + \tau_{\mathrm{sl}0} = 0$, then $h_{y0} = h/2$. In pure bending loaded state, $h_y = h/2$. By substituting equation (11) into equation (10), we can see that the height of neutral axis h_y does not affect the surface residual stress, the height of neutral axis, and the curvature in relaxed state. Therefore, the choice of reference or relaxed configuration does not influence the bending deformation of nanowire.

Equation (8) indicates that flexural rigidity is composed of three parts. The first term is defined by the precept of continuum mechanics, and the last two terms are defined by surface elasticity. We can also conjecture that the positive GM and SO constants will increase the flexural rigidity, whereas the negative ones will decrease the rigidity of nanowire. Figure 3 presents the normalized curvature ($12\kappa_y/Ebh^3$) versus the height of the ⟨1 1 0⟩ axially oriented nanowire. The figure shows that the normalized curvature also increases with the decrease in height, thereby stiffening the nanowire. For a 2 nm-high nanowire, its curvature changes by 8.2% when SO and GM corrections are applied. Notably, the bending curvature (κ_y) is independent of the surface residual stress. It is the relaxation curvature of nanowire (κ_{y0}) that is influenced by the surface residual stress. For the isotropic circular nanowire without surface residual stress, the components of rigidity are the same as the rectangular nanowire. We also find the stiffening effect for the positive SO and GM constants and the reverse for negative constants.

4. Conclusions

In this work, simple beam theory and curvature-dependent surface elasticity are adopted to capture the flexural properties of nanowire. Surface tension is depicted by the GM model, and surface couple stress is depicted by the SO model. Following the work of Chhapadia et al., we divide the bending deformation of nanowire into the reference and relaxed states. We obtain the expressions of bending curvature and height of neutral axis by using the internal force balance of simple beam with the effect of surface stress. In the relaxed state, the relaxation bending curvature caused by the surface residual stress difference between the upper and lower faces relates to the height of nanowire and the SO constant. The bending rigidity increases with the decrease in the height of nanowire and the positive SO constant. In particular, the height of neutral axis will be half of the height of nanowire if the surface residual stress on the upper and lower surfaces is asymmetrically distributed along the axial direction. In the pure bending moment state, the bending curvature relates to the height of nanowire and the GM and SO constants. The bending rigidity also increases with the decrease in the height of nanowire and the positive GM and SO constants, thereby stiffening the nanowire. Therefore, not only sizes and elastic modulus of bulk material but also relaxation surface curvature induced by surface residual stress influence the bending rigidity of nanowire.

Data Availability

The cited data about surface elastic constants of silver nanowire used to support the findings of this study are included within the referenced article. These data were used to verify our theoretical prediction.

Conflicts of Interest

The authors declare that they have no conflicts of interest.

Acknowledgments

The authors gratefully acknowledge the financial support provided by the National Engineering Laboratory for Highway Tunnel Construction Technology (grant no. NELFHT201702) and Key Research Project of Xihua University (grant no. z1320608).

References

[1] D. Appell, "Wired for success," *Nature*, vol. 419, no. 6907, pp. 553–555, 2002.

[2] E. Gil-Santos, D. Ramos, J. Martínez et al., "Nanomechanical mass sensing and stiffness spectrometry based on two-dimensional vibrations of resonant nanowires," *Nature Nanotechnology*, vol. 5, no. 9, pp. 641–645, 2010.

[3] S. Wang, Z. Shan, and H. Huang, "The mechanical properties of nanowires," *Advanced Science*, vol. 4, no. 4, Article ID 1600332, 2017.

[4] M. E. Gurtin and A. Ian Murdoch, "A continuum theory of elastic material surfaces," *Archive for Rational Mechanics and Analysis*, vol. 57, no. 4, pp. 291–323, 1975.

[5] R. E. Miller and V. B. Shenoy, "Size-dependent elastic properties of nanosized structural elements," *Nanotechnology*, vol. 11, no. 3, pp. 139–147, 2000.

[6] W. Zhang, T. Wang, and X. Chen, "Effect of surface stress on the asymmetric yield strength of nanowires," *Journal of Applied Physics*, vol. 103, no. 12, Article ID 123527, 2008.

[7] G.-F. Wang and X.-Q. Feng, "Effects of surface elasticity and residual surface tension on the natural frequency of microbeams," *Applied Physics Letters*, vol. 90, no. 23, Article ID 231904, 2007.

[8] F. Xu, Q. Qin, A. Mishra, Y. Gu, and Y. Zhu, "Mechanical properties of ZnO nanowires under different loading modes," *Nano Research*, vol. 3, no. 4, pp. 271–280, 2010.

[9] D. J. Steigmann and R. W. Ogden, "Elastic surface substrate interactions," *Proceedings of the Royal Society of London*, vol. 455, no. 1982, pp. 437–474, 1999.

[10] P. Chhapadia, P. Mohammadi, and P. Sharma, "Curvature-dependent surface energy and implications for nanostructures," *Journal of the Mechanics and Physics of Solids*, vol. 59, no. 10, pp. 2103–2115, 2011.

[11] X. Gao, Z. Huang, J. Qu, and D. Fang, "A curvature-dependent interfacial energy-based interface stress theory and its applications to nano-structured materials: (I) general theory," *Journal of the Mechanics and Physics of Solids*, vol. 66, pp. 59–77, 2014.

[12] P. Gupta and A. Kumar, "Effect of surface elasticity on extensional and torsional stiffnesses of isotropic circular nanorods," *Mathematics and Mechanics of Solids*, vol. 24, no. 6, pp. 1613–1629, 2019.

[13] H. Y. Yao, G. H. Yun, N. Bai, and J. G. Li, "Surface elasticity effect on the size-dependent elastic property of nanowires," *Journal of Applied Physics*, vol. 111, no. 8, Article ID 083506, 2012.